

Quantifying stochastic outcomes

Gareth Baxter and Alan J. McKane

Theory Group, School of Physics and Astronomy, University of Manchester, Manchester M13 9PL, United Kingdom

Martin B. Tarlie

Complex Systems Group, Northwestern University, 2145 Sheridan Road, Evanston, Illinois 60208, USA

(Received 17 July 2004; published 13 January 2005)

A system consisting of two species in a fluctuating environment, when the interspecies competition for resources is strong, will have a stochastic outcome: only one of the species will survive, but there is no *a priori* way of knowing which one this will be. It is natural in such a situation to ask what will be the probability of one or another of the species surviving. This probability is calculated as a function of the average growth rates and the strengths of the interaction between the species and of the randomness. This is an example of a class of stochastic problems in which multiple final states are available for occupation. We refer to the choice of final states as state selection, and the probabilities of final states being occupied as state-selection probabilities. The calculation of these probabilities is carried out in the context of a model of the system which consists of two coupled stochastic differential equations. By reformulating these equations in terms of path integrals, the powerful methods based on the use of optimal paths may be utilized to calculate the probability of one outcome or the other. The analytical results obtained by using this technique agree well with numerical simulations when both species have the same growth rate. Although the method adopted rests on the assumption that the strength of the fluctuations, D , is small, remarkably the analytic results are still found to be in good agreement with the numerical results when D is of order 1.

DOI: 10.1103/PhysRevE.71.011106

PACS number(s): 05.40.Ca, 87.23.Cc, 05.10.Gg

I. INTRODUCTION

The dynamics of interacting species has been extensively studied over many years and has a huge literature associated with it. The models proposed to describe the dynamics are extremely varied. For example, they may be deterministic or stochastic, focus on the realistic modeling of the interactions between the species, stress the role of special relationships between the species (for instance, host-parasite), or investigate the possible generalizations to multispecies communities. In this paper, we will be mainly concerned with the effect of stochasticity from external sources, and will therefore keep other complicating factors to a minimum. We will study a system comprising two species, with populations $N_1(t)$ and $N_2(t)$ at time t , which have growth rates r_1 and r_2 , respectively, in the absence of interaction between individuals. The interaction induced due to competition for resources will reduce these growth rates by (i) intraspecies competition, which will be assumed to be proportional to the number of individuals in the species under consideration, and (ii) interspecies competition, which will be assumed to be proportional to the number of individuals of the other species.

This is one of the simplest models for competition between two species, usually called the Lotka-Volterra (LV) competition model [1]. The deterministic version of the model is defined by the following two coupled ordinary differential equations:

$$\frac{dN_1}{dt} = N_1(r_1 - a_{11}N_1 - a_{12}N_2), \quad (1)$$

$$\frac{dN_2}{dt} = N_2(r_2 - a_{22}N_2 - a_{21}N_1). \quad (2)$$

The parameters of the model, r_i, a_{ij} ; $i, j=1,2$, are all assumed to be positive. In the absence of the interspecies interaction parameters a_{12} and a_{21} , both species would separately follow logistic growth, with species i achieving an equilibrium population of r_i/a_{ii} individuals at long times. The inclusion of the a_{12} and a_{21} factors may still allow coexistence, but with different equilibrium population sizes, but it may also cause one of the species to die out. This is well known [1] and is briefly reviewed in the next section.

In many ways, Eqs. (1) and (2) can be said to represent the minimal model which takes competition into account between two species. We have already mentioned several ways in which it could be extended. In this paper, we will be interested in the introduction of environmental stochasticity. The philosophy of the approach is as follows. The important aspects we wish to model (in this case the dynamics of the two species) are given by a set of deterministic equations [in this case Eqs. (1) and (2)]. These should capture the essentials of the interaction in the absence of any other factors. In reality, external factors such as climate, terrain, the presence of other species, indeed any factor which may have a small uncertain influence on the two species should all have an effect. Since we cannot possibly model all of these complex factors in detail, the best we can do in a simple model is to regard them as random—if we did try to systematically model them, we would be looking at a much more complicated deterministic system. This way of modeling the system leads to governing equations which are stochastic, rather than deterministic.

The external effects are incorporated into Eqs. (1) and (2) in the same way that the competitive effects were: the growth rates are modified by including a stochastic term [2]. Thus the deterministic growth rate $r_1 - a_{11}N_1 - a_{12}N_2$ in Eq. (1) is replaced by the stochastic growth rate $r_1 - a_{11}N_1 - a_{12}N_2 + \eta_1(t)$, with the addition of a similar term, $\eta_2(t)$, in Eq. (2). Since the $\eta_i(t)$ are designed to reflect a large number of coupled variables omitted from the description of the model, it is natural, by virtue of the central limit theorem, to assume that the $\eta_i(t)$ are Gaussianly distributed. It also seems realistic to assume that any temporal correlation between these external influences is on scales very much shorter than those of interest to us here and that the $\eta_i(t)$ have zero mean. We therefore assume that

$$\langle \eta_i(t) \eta_j(t') \rangle = 2D_i \delta_{ij} \delta(t - t'), \quad i, j = 1, 2, \quad (3)$$

where δ_{ij} and $\delta(t - t')$ are the Kronecker and Dirac delta functions, respectively. The D_i are constants which describe the strength of the stochastic effects. Since the $\eta_i(t)$ are Gaussian, the definitions (3) and the fact that they have zero mean [$\langle \eta_i(t) \rangle = 0$, $i = 1, 2$] imply that the stochastic process is now completely specified. Therefore, the statistics of the $N_i(t)$ —which are now themselves stochastic processes—can be determined from the stochastic versions of Eqs. (1) and (2),

$$\frac{dN_1}{dt} = N_1[r_1 - a_{11}N_1 - a_{12}N_2 + \eta_1(t)], \quad (4)$$

$$\frac{dN_2}{dt} = N_2[r_2 - a_{22}N_2 - a_{21}N_1 + \eta_2(t)]. \quad (5)$$

The stochastic, or noise, terms are multiplicative: they appear multiplying a function of N_1 and N_2 .

Coupled differential equations of the type that appear in the deterministic LV model cannot, in general, be solved exactly, so it is not surprising that coupled stochastic differential equations such as Eqs. (4) and (5) are even harder to analyze. In the past, the analysis of the stochastic model has been almost entirely numerical, frequently with the inclusion of addition effects such as colored noise, periodic fluctuations, or spatial effects [3–11]. Considerable progress on what is probably the most important question in these kinds of models—the eventual fate of the two populations at large times—may be made in the deterministic case with almost no calculation [1]. On the other hand, one of the most important new features that occurs when going from the deterministic model to the stochastic model is that in the stochastic model it is no longer true that a given initial condition leads to the same outcome on every occasion. We now have to speak about the probability of species 1 dying out or the probability of species 1 surviving. When the stochastic LV model is completely specified (that is, both the parameters in the deterministic equations are given and the statistics of the fluctuations is fixed), these probabilities are well defined quantities. They can, for instance, be found by numerically solving a large number of realizations of the process, and counting the proportion of the runs in which either species 1 or species 2 becomes extinct.

In this paper, we will describe a scheme for calculating these probabilities analytically. More specifically, we will choose the parameter range in the LV model for which the coexistence equilibrium state is unstable, and so eventually either species 1 or species 2 will die out. We will then calculate the probability of these occurrences as a function of the parameters of the model. The calculation will be carried out in the limit of weak external effects ($D_1, D_2 \rightarrow 0$) using a path-integral representation which holds for equations of the type (4) and (5). The power of this approach is that, while approximation techniques for stochastic differential equations are difficult, these equations may be represented as path integrals *without approximation* and then systematic approximation techniques for path integrals developed over the years can be utilized. These methods are valid in the limit of weak fluctuations, but since these extraneous effects are assumed to be small random perturbations, this seems entirely reasonable. We have discussed the general aspects of these kinds of calculations elsewhere [12–14] and have also discussed this particular problem in a general way [15]. In fact, the current paper may be thought of as following on from Ref. [15], where the strength of the path-integral method is emphasized and the point illustrated on systems of one variable. The calculation involving systems of two variables is sketched out in that paper, but no details of the background to the model considered or of the calculations required are given. In the present paper, we will therefore concentrate on giving some background to the study and we also explain the details of the calculation.

This use of stochastic differential equations for modeling purposes has a long history in the physical sciences (for example, the use of the Langevin equation to study Brownian motion [16,17]) but is much less common in the biological sciences. The equations we have described were first formulated by May [2,18]. Stochastic differential equations which contain multiplicative noise, such as these, have some subtle aspects which must be treated carefully [19]. This has been understood, and discussed in detail, by some biologists [20]. Fortunately, we will obtain excellent agreement with simulation results by performing only a leading-order calculation in the noise strength. Since any subtleties associated with the occurrence of multiplicative noise only manifest themselves at next to leading order, we will not need to confront these issues here. The system of Eqs. (1) and (2) does not constitute a potential model (they cannot be written in the form $\dot{N}_1 = -\partial V / \partial N_1$, $\dot{N}_2 = -\partial V / \partial N_2$, for some V). Although this does not pose a problem for the application of our method, a potential model makes it easier to visualize some of the processes involved, and to draw analogies with physical processes such as a Brownian particle moving on a surface. We will therefore introduce another model which resembles the Lotka-Volterra competition model (LVCM), but which is derivable from a potential and which has additive noise, rather than multiplicative noise. We will call this the additive noise potential model (ANPM). It will turn out that the analyses of these two models are so closely related that they may be carried out in parallel.

The outline of the paper is as follows. In Sec. II, we find the equilibrium states and introduce variants of the model.

The technique we use to perform calculations is introduced in Sec. III and implemented in the cases of interest to us in Secs. IV and V. The results are also given in Sec. V, where they are compared with the results of Monte Carlo simulations. Our conclusions are given in Sec. VI. Three Appendixes describe technical details associated with the determination of the optimal paths and the calculation of the actions of these paths.

II. MODELS

In this section, we will review the nature of the equilibrium states of the deterministic model. While these results are well known, the analysis and associated discussion is necessary to enable us to describe the qualitative aspects of state selection in more detail. We will also define the reduced model, which contains the essential elements of the full model, and the ANPM, which consists of a set of equations which are easier to visualize and which display the same phenomenon of state selection.

Our main aim in this paper is to illustrate how techniques based on path integrals can be used to make analytical progress in the investigation of stochastic models of population dynamics. The technique is applicable in a wide range of situations, the only real requirement being that the strengths of the fluctuations are small. This can be implemented by writing $D_1 = \rho_1 D$ and $D_2 = \rho_2 D$, where ρ_1 and ρ_2 are constants of order 1, which are to be considered part of the set of the parameters of the model in the same way that the r_i and the a_{ij} are, and D is the small parameter used in the approximation as described in the next section. Although the formalism is applicable to far more complicated models than that of LV, and with an arbitrary number of species, we will try to make the analysis as transparent as possible by looking at the case where $\rho_1 = \rho_2$ and $a_{12} = a_{21}$. This corresponds to the situation where the two species have a symmetric effect on each other and are affected by external factors equally strongly. We can simplify notation for this choice by writing $D_1 = D_2 = D$, $r_1 = \alpha$, $r_2 = \beta$, $a_{12} = a_{21} = \gamma$, $a_{11} = \delta$, $a_{22} = \epsilon$, $N_1(t) = x(t)$, and $N_2(t) = y(t)$, so that the model now reads

$$\dot{x} = \alpha x - \gamma xy - \delta x^2 + x \eta_1(t), \quad (6)$$

$$\dot{y} = \beta y - \gamma xy - \epsilon y^2 + y \eta_2(t), \quad (7)$$

where the dot denotes differentiation with respect to time and where

$$\langle \eta_i(t) \rangle = 0, \quad \langle \eta_i(t) \eta_j(t') \rangle = 2D \delta_{ij} \delta(t - t'), \quad i, j = 1, 2. \quad (8)$$

The model defined by Eqs. (6)–(8) encompasses situations where the two species coexist for long periods as well as situations where either one or the other dies out. To explore this, let us first consider the deterministic case. The equilibrium states are solutions of

$$0 = x(\alpha - \gamma y - \delta x), \quad (9)$$

$$0 = y(\beta - \gamma x - \epsilon y). \quad (10)$$

An unstable solution at the origin always exists; the other solutions are either stable or of mixed stability (one stable direction and one unstable direction), that is, saddle points. They are as follows:

1(a). $(x, y) = (\alpha/\delta, 0)$, which is stable if $\alpha\gamma > \beta\delta$ and a saddle if $\alpha\gamma < \beta\delta$.

1(b). $(x, y) = (0, \beta/\epsilon)$, which is stable if $\beta\gamma > \alpha\epsilon$ and a saddle if $\beta\gamma < \alpha\epsilon$.

2. Since $x, y > 0$, a solution with $x \neq 0$, $y \neq 0$ will only exist if $\alpha\gamma - \beta\delta$, $\beta\gamma - \alpha\epsilon$ and $\gamma^2 - \delta\epsilon$ all have the same sign. It will then be given by

$$(x, y) = \left(\frac{\beta\gamma - \alpha\epsilon}{\gamma^2 - \delta\epsilon}, \frac{\alpha\gamma - \beta\delta}{\gamma^2 - \delta\epsilon} \right). \quad (11)$$

This solution is stable if $\gamma^2 < \delta\epsilon$ and a saddle if $\gamma^2 > \delta\epsilon$.

All of this is well known [1], and it is reviewed here simply as a foundation on which to build our discussion of the qualitative behavior of the stochastic model. For this reason, we have omitted the situations in which there are accidental degeneracies [e.g., $\alpha\gamma = \beta\delta$ in 1(a)]. We determined the stabilities of the equilibrium states by linear stability analysis, although a simple global stability analysis is available in most cases (see below).

Based on the above, three different types of behavior are possible, depending on the parameters of the model.

I. If $\alpha\gamma - \beta\delta$ (or $\beta\gamma - \alpha\epsilon$) is of opposite sign to $\gamma^2 - \delta\epsilon$, then no solution of type 2 exists and only one of the solutions 1(a) and 1(b) is stable. If 1(a) is stable, then species y will always die out, and x will survive, and vice versa if 1(b) is stable.

II. If $\alpha\gamma < \beta\delta$ and $\beta\gamma < \alpha\epsilon$ ($\Rightarrow \gamma^2 < \delta\epsilon$), a solution of type 2 exists and is stable. The two equilibrium points on the axes are no longer stable. The final state is therefore given by Eq. (11).

III. If $\alpha\gamma > \beta\delta$ and $\beta\gamma > \alpha\epsilon$ ($\Rightarrow \gamma^2 > \delta\epsilon$), a solution of type 2 exists but is now no longer stable. The two equilibrium points on the axes are stable in this case. The final state consists of individuals which belong either to species x or species y .

While the stochastic version of all these cases is interesting, the first two differ from the last in that there is only one stable equilibrium state. Thus while the stochastic dynamics will differ from the deterministic dynamics in many details in these two cases, the final state will usually be the same as found in the deterministic case. Even in case II, where the system may leave the “final” state through fluctuations, the most likely outcome will be coexistence of species [2]. This is not true for case III. This case is already different in the deterministic LV model, because unlike cases I and II, a global stability analysis is not possible [1]. Therefore, one cannot use simple arguments in the deterministic case III to predict what the final state will be (whether the x or y species will become extinct) for given initial populations of species x and species y . The final states are, of course, known with certainty given the initial states: the stable stationary solutions $(\alpha/\delta, 0)$ and $(0, \beta/\epsilon)$ will have basins of attraction which can be crudely characterized as “large x , small y ” and

“large y , small x ,” or the “ x valley” and “ y valley,” respectively. In the deterministic problem, the initial starting point determines absolutely the final selected state—they are in the same basin of attraction. These two basins will be separated by a line—the separatrix—which runs from the origin through the saddle point given by Eq. (11) (or by the corresponding expression in the reduced model). Although the equation of the separatrix may be found, without knowing its exact position it is not possible to decide in any simple way whether initial points close to the separatrix are in the basin of attraction of one fixed point or the other. For the stochastic version of the model, on the other hand, there is a nonzero probability that the system may move out of the basin of attraction in which it starts and into the other one. It is this probability that we wish to calculate.

From the discussion so far in this section, we may describe qualitatively the expected behavior of $x(t)$ and $y(t)$ starting at the initial point (x_0, y_0) at $t=0$. The situation which is of interest to us, case III, is characterized by interspecies competition (with a strength given by γ), which is strong as compared to intraspecies competition (with strengths δ and ϵ for species x and y , respectively). A direct consequence of this is that the stable states on the x and y axes are further out from the origin, in both the x and y directions, than is the saddle point. We can guarantee to be in this regime by supposing that δ and ϵ are very small, so that the stable states are now at very large values of x and y . Since these solutions are just at the stationary values of the logistic equation for the successful species, this simply corresponds to a large carrying capacity for the two species. By contrast, the position of the unstable state has changed much less: in the limit where δ and ϵ go to zero, the coordinate of this equilibrium state tends to the finite value $(\beta/\gamma, \alpha/\gamma)$, whereas the stable states tend to infinity.

Since our main aim in this paper is to present a method for calculating the probabilities of either species x or species y being selected as the survivor, and since the essential features become much clearer in the limit $\delta, \epsilon \rightarrow 0$, we will work in this limit for the rest of the paper. We call this the reduced problem and its relation to the full problem has been discussed extensively in one of our earlier papers [14]. It is defined by

$$\dot{x} = \alpha x - \gamma xy + x \eta_1(t), \quad (12)$$

$$\dot{y} = \beta y - \gamma xy + y \eta_2(t), \quad (13)$$

where $\eta_i(t)$ is a Gaussian noise specified by Eq. (8).

The deterministic reduced LV model has only two equilibrium states: the unstable state at $(0, 0)$ and the saddle point at (x^*, y^*) , where

$$x^* = \frac{\beta}{\gamma}, \quad y^* = \frac{\alpha}{\gamma}. \quad (14)$$

Since there is now no stable state, we will consider one species to have been selected as the survivor when the system has moved far enough from the origin that the probability of returning is negligible.

The formulation we have just described applies to any set of first-order equations which are acted upon by Gaussian white noise. The model defined by Eqs. (6) and (7), or alternatively Eqs. (12) and (13), is of primary interest to us, but has two technical complications associated with it. First, in its deterministic form (that is, in the absence of noise) it is not a potential problem. This means that there is no potential $V(x, y)$ whose minima correspond to stable fixed points and whose maxima correspond to unstable fixed points. Secondly, the noise is multiplicative. One consequence of this is that the stochastic differential equations (6) and (7) are ambiguous as they stand; further information has to be given to make the problem well-posed [19] (although, as we mentioned in the Introduction, this ambiguity will not manifest itself to the order at which we are working). For these reasons, we will also study a set of equations which resemble Eqs. (6) and (7), but which do not suffer from these difficulties, namely

$$\dot{x} = \alpha x - \gamma xy^2 - \delta x^3 + \eta_1(t), \quad (15)$$

$$\dot{y} = \beta y - \gamma x^2 y - \epsilon y^3 + \eta_2(t), \quad (16)$$

or the reduced version with $\delta = \epsilon = 0$. Once again, it corresponds to the situation where the locally stable states are pushed out to infinity and the state selection now occurs when the system reaches one of the infinitely long valleys leading to these states. Since the state selection occurs before the system reaches the vicinity of the stable states, this is expected to have little influence on the phenomenon of state selection—as can be easily observed from a study of the trajectories in Monte Carlo simulations [14]. Equations (15) and (16) may be written in the form

$$\dot{x} = -\frac{\partial V}{\partial x} + \eta_1(t), \quad (17)$$

$$\dot{y} = -\frac{\partial V}{\partial y} + \eta_2(t), \quad (18)$$

with

$$V(x, y) = -\frac{\alpha}{2}x^2 - \frac{\beta}{2}y^2 + \frac{\gamma}{2}x^2y^2 + \frac{\delta}{4}x^4 + \frac{\epsilon}{4}y^4. \quad (19)$$

For the reduced model

$$V_R(x, y) = -\frac{\alpha}{2}x^2 - \frac{\beta}{2}y^2 + \frac{\gamma}{2}x^2y^2. \quad (20)$$

This is the ANPM.

In the absence of noise, the stationary points of the system occur when $\partial V/\partial x = 0$ and $\partial V/\partial y = 0$. They are an unstable local maximum at the origin and four saddle points between the axes at

$$x^* = \pm \sqrt{\frac{\beta}{\gamma}}, \quad y^* = \pm \sqrt{\frac{\alpha}{\gamma}}. \quad (21)$$

These points are marked in Fig. 1, which is a plot of the potential (on the vertical axis) for a particular choice of parameters. Such a figure cannot be drawn for the nonpotential

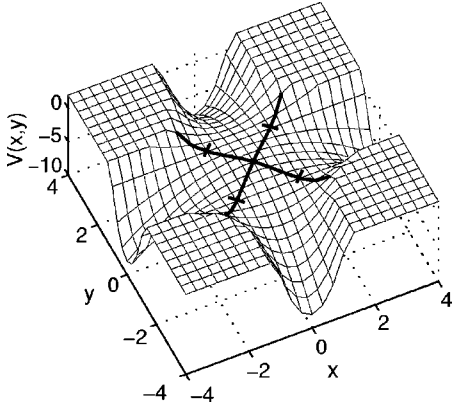


FIG. 1. Representation of the potential V_R defined by Eq. (20), with $\alpha=\beta=\gamma=1$. The saddle points (+) and separatrices (heavy lines) are also marked.

LVCM. In the ANPM, negative valued states are accessible, which means there are four final states that can be selected, corresponding to the four “valleys” in the potential that lie along the axes. Without noise, the system is entirely deterministic, and just as for the LVCM, the x - y plane can be divided into the basins of attraction of these states.

We have seen that all of the models in this section show state selection: there are two or more possible final states, and we can only give the probability that one of these states will be selected in a given realization. A method which allows us to calculate this probability will be discussed in the next section.

III. PATH INTEGRALS

In this section, we review the formulation of stochastic differential equations, such as Eqs. (12) and (13) or Eqs. (17) and (18), as path integrals and obtain the dominant contribution to the conditional probability we wish to determine in the limit where the noise strength tends to zero.

Instead of attempting to solve stochastic differential equations of the kind we have been discussing in this article, another way of proceeding is to simply imagine carrying out a large number of simulations of the stochastic equations, each with a different realization of the $\eta_i(t)$ and all starting at $\vec{r}_0=(x_0,y_0)$ at $t=0$. Each simulation gives a different path $\vec{r}(t)=(x(t),y(t))$, and to calculate the expected value of a given quantity we simply multiply it by the Gaussian probability factor $\exp\{-(1/4D)\int dt[\eta_1^2(t)+\eta_2^2(t)]\}$, and integrate over all $\eta_1(t)$ and $\eta_2(t)$. The simplest quantity to consider is the conditional probability that the system is in the state (x_f,y_f) at time T , given it was initially in the state (x_0,y_0) at $t=0$. In this case, we simply have to pick out only those paths which pass through the point $\vec{r}_f=(x_f,y_f)$ at time T . This is the path-integral representation for Gaussian stochastic processes [21–23]. Focusing for the moment on the LVCM, we can change variables from the $\eta_i(t)$ to the actual path coordinates $x(t)$ and $y(t)$ given by Eqs. (12) and (13). Apart from a Jacobian factor, J , arising from the change of variables [24], the conditional probability is then simply the sum

over all these paths weighted with the factor deriving from the Gaussian distribution,

$$P(\vec{r}_f,T|\vec{r}_0,0) = \mathcal{C} \int_{\vec{r}(0)=\vec{r}_0}^{\vec{r}(T)=\vec{r}_f} D\vec{r} J[\vec{r}] \exp\{-S[\vec{r}]/D\}, \quad (22)$$

where \mathcal{C} is a normalization constant and where

$$S[\vec{r}] = \frac{1}{4} \int_0^T dt \left[\left(\frac{\dot{x}}{x} - \alpha + \gamma y \right)^2 + \left(\frac{\dot{y}}{y} - \beta + \gamma x \right)^2 \right]. \quad (23)$$

The functional $S[\vec{r}]$ given by Eq. (23) is specific to the reduced LVCM and is obtained by eliminating $\eta_1(t)$ and $\eta_2(t)$ from the Gaussian probability factor given above by using Eqs. (12) and (13). The expression in Eq. (22) is the path-integral representation of the model. It has the same content as Eqs. (8), (12), and (13), and forms the basis of our method. Just as ordinary integrals of the form $\int_a^b dr g(r) \exp\{f(r)/D\}$ may be evaluated by the method of steepest descent in the limit $D \rightarrow 0$, so functional integrals of the type (22) may also be evaluated this way. For $D \rightarrow 0$, the path integral (22) is dominated by solutions of the differential equations $\delta S / \delta \vec{r}(t) = 0$, which satisfy the boundary conditions $\vec{r}(0) = \vec{r}_0$ and $\vec{r}(T) = \vec{r}_f$. Just as for $g(r)$ in the ordinary integral case, the specific form for the functional $J[\vec{r}]$ is only important at next to leading order. As we will see, a leading-order calculation is sufficient to give very accurate results, so we will not consider $J[\vec{r}]$ further in this paper.

This formalism is very reminiscent of the variational formulation of classical mechanics [25] and so, by analogy, $S[\vec{r}]$ is called the action, and sometimes we attach a subscript “ c ” to the solutions of the Euler-Lagrange equations $\delta S / \delta \vec{r}(t) = 0$, to indicate that they are “classical” paths. However, we will follow common usage and call them *optimal paths* and frequently omit the subscript “ c ” when it is clear that optimal paths are being considered. The result of performing the functional steepest descent on Eq. (22) to leading order gives

$$P(\vec{r}_f,T|\vec{r}_0,0) \sim \exp\{-S_c(\vec{r}_f,T;\vec{r}_0)/D\}, \quad (24)$$

where S_c is just the action of the optimal path $\vec{r}_c(t)$. The result (24) is the starting point for our method: if we can determine the function S_c , then we will have a form for the conditional probability valid when the noise is weak. This in turn will enable us to obtain a formula for the probability that either species y becomes extinct or species x becomes extinct, as a function of α , β , γ , and D .

The quantity $S[\vec{r}]$, sometimes also called the Onsager-Machlup functional [22,23,26], plays a central role in the theory of stochastic processes when they are expressed by equations such as Eqs. (12) and (13). When the problem under consideration is a potential problem, such as the ANPM, defined by Eqs. (17) and (18), it takes on an especially simple form,

$$S[\vec{r}] = \frac{1}{4} \int_0^T dt \left[\left(\dot{x} + \frac{\partial V}{\partial x} \right)^2 + \left(\dot{y} + \frac{\partial V}{\partial y} \right)^2 \right], \quad (25)$$

which may also be written as

$$S[\vec{r}] = \frac{1}{2} \int_0^T dt \left[\frac{1}{2} (\dot{x}^2 + \dot{y}^2) - U(x, y) \right] + \frac{1}{2} \int_0^T dt \frac{dV}{dt}, \quad (26)$$

where

$$U = -\frac{1}{2} \left(\frac{\partial V}{\partial x} \right)^2 - \frac{1}{2} \left(\frac{\partial V}{\partial y} \right)^2. \quad (27)$$

The form (26) is useful because the last term is simply $(1/2)\Delta V$, and so only depends on the boundary values. This means that a variation of Eq. (26) to obtain the optimal path gives the same equations as those for a classical particle of unit mass moving in a two-dimensional potential given by Eq. (27).

IV. OPTIMAL PATHS

So far we have reformulated the stochastic differential equations (12) and (13), or those associated with the potential (19), as functional integrals, and explained that as $D \rightarrow 0$ these integrals will be dominated by the solutions of the equations $\delta S / \delta \vec{r}(t) = 0$. These are the optimal paths of the problem. In this section, we will obtain explicit forms for the equations satisfied by the optimal paths and obtain approximate solutions for them.

For a potential problem, the variation of the action (26) gives

$$\ddot{x} = -\frac{\partial U}{\partial x}, \quad (28)$$

$$\ddot{y} = -\frac{\partial U}{\partial y}, \quad (29)$$

where $U(x, y)$ is given by Eq. (27). These are Newton's law, but in the potential, U , not in the original potential of the stochastic problem, V . It is important to realize that there are two distinct dynamics associated with the problem under consideration. The first is the stochastic dynamics given by the stochastic differential equations with the potential $V(x, y)$. This was our starting point, and is the basis of discussions invoking Brownian particles and is the dynamics of Monte Carlo simulations. The second dynamics is the *deterministic* dynamics given by Eqs. (28) and (29), which describe the $D \rightarrow 0$ limit of the stochastic dynamics. They are quite different and one should not transfer intuition from one to the other without great care being taken.

The potential U for the full ANPM is obtained from Eqs. (19) and (27) to be

$$U(x, y) = -\frac{1}{2} x^2 (\alpha - \gamma y^2 - \delta x^2)^2 - \frac{1}{2} y^2 (\beta - \gamma x^2 - \epsilon y^2)^2. \quad (30)$$

For the reduced problem, which we will concentrate on in this paper, this potential becomes

$$U_R(x, y) = -\frac{1}{2} x^2 (\alpha - \gamma y^2)^2 - \frac{1}{2} y^2 (\beta - \gamma x^2)^2. \quad (31)$$

From Eqs. (28) and (29), but using the reduced potential U_R , we obtain the explicit equations for the optimal paths to be

$$\ddot{x} = x(\alpha - \gamma y^2)^2 - 2\gamma x y^2 (\beta - \gamma x^2), \quad (32)$$

$$\ddot{y} = y(\beta - \gamma x^2)^2 - 2\gamma y x^2 (\alpha - \gamma y^2). \quad (33)$$

Of course, this additive noise potential model was introduced as a simpler system which nevertheless contains the same phenomena as the LV competition model, which is the real focus of our interest. Since there is no potential for the LV model, we have to obtain the equations for the optimal paths directly from a variation of Eq. (23). One finds

$$\frac{1}{x} \frac{d}{dt} \left(\frac{\dot{x}}{x} - \alpha + \gamma y \right) = \gamma \left(\frac{\dot{y}}{y} - \beta + \gamma x \right), \quad (34)$$

$$\frac{1}{y} \frac{d}{dt} \left(\frac{\dot{y}}{y} - \beta + \gamma x \right) = \gamma \left(\frac{\dot{x}}{x} - \alpha + \gamma y \right). \quad (35)$$

It should be noted that whereas the first set of equations (32) and (33) are Newton's equations for a particle of unit mass moving without friction in the potential U_R , the second set of equations (34) and (35) have no such simple interpretation. Both sets of equations are to be solved for paths satisfying the initial and final conditions

$$x(0) = x_0, \quad y(0) = y_0 \quad (36)$$

$$x(T) = x_f, \quad y(T) = y_f. \quad (37)$$

We will study both sets of equations in parallel since, although they look rather different, the method we adopt when solving them will bring out their similarities.

Our starting point is the observation that the stochastic effects are only significant in the vicinity of the separatrix. Thus we only need to find the optimal paths for initial conditions which are close to the separatrix; the final state is determined with probability very nearly 1 for initial conditions sufficiently far from the separatrix. The final states are the “ x -valley” and “ y -valley” basins in both cases. To calculate the probability of ending up in these states, an integration over each basin will need to be carried out.

The choice of the time interval between the initial and final states is more subtle. Let us imagine starting many realizations of the stochastic system at the same position near to the separatrix. After some time, T , most of the systems will be approaching the final state which is on the same side of the separatrix as the initial state. The remaining systems will be approaching the final state on the other side of the separatrix. Nevertheless, in both cases the system will have “chosen” one of the states as long as T is reasonably large. Increasing T beyond this value will not change the fraction of systems which choose one state or the other. Therefore, we may choose T to have any value, as long as state selection has had a chance to occur, and in fact it will be convenient to take $T \rightarrow \infty$.

The nature of the optimal paths for large T was discussed in Ref. [15] in some detail for the one-dimensional stochastic problem defined by $\dot{x} = -V'(x) + \eta(t)$, where $V(x)$ is a potential with a single maximum at $x=0$ such as $V(x) = -(\alpha/2)x^2$. For the moment, we only need to use the fact that, in the mechanical analogy of the deterministic motion of a particle of unit mass, the only way that the particle can reach a finite final state after a very large time is if its path takes it very close to the saddle point. This is the only region where it can effectively be trapped for an infinite length of time (in the limit $T \rightarrow \infty$). The analog in the one-dimensional problem is paths which approach very near to the maximum of the potential. We can now explain why taking the large time limit is advantageous: if we did not do so, we would have to solve two coupled nonlinear equations such as Eqs. (32) and (33) or Eqs. (34) and (35) between two arbitrary points—an extremely difficult task. On the other hand, when $T \rightarrow \infty$, the optimal path can be broken down into two pieces. The first part will be from (x_0, y_0) to the saddle point, the second from the saddle point to the final point (x_f, y_f) . Since one of the end points of both paths is the saddle point (in the limit $T \rightarrow \infty$), the problem of solving the differential equations becomes tractable.

As we will see, we need to keep T large but finite in order to calculate the probability, letting $T \rightarrow \infty$ at the end of the calculation. We still divide the path into two parts, but with some care. One part contains most of the motion from the initial point to the saddle. The second part, which contains the motion from the saddle to the end point, is very small for times before the saddle is reached. For finite T , the optimal path never exactly reaches the saddle point. To account for this, we incorporate a small offset into the second part of the path, which then begins at some small finite value at $t=0$ and ends at (x_f, y_f) at $t=T$. As $T \rightarrow \infty$, this initial value tends to zero. The first part of the path then does not start exactly at (x_0, y_0) , but the sum of the initial points of the two sections will be (x_0, y_0) . The action we calculate for the first section of the path will differ from the infinite T value only by exponentially small corrections. In the rest of this section, we will concentrate on finding the equations and action for the first part of the path in the limit $T \rightarrow \infty$. In Sec. V, we will describe the division of the path more precisely and discuss why the details of the second part of the path are far less important.

To determine the optimal path from (x_0, y_0) to the saddle point, we need to determine the equation of the separatrix, since we will be treating initial conditions near to the separatrix in a different way from those which are not. The equation of the separatrix can be found by determining the trajectories of the system with no noise which pass through the saddle points. For the ANPM, the equations for these trajectories are

$$\dot{x} = \alpha x - \gamma xy^2, \quad \dot{y} = \beta y - \gamma yx^2, \quad (38)$$

which leads to the following equation for the separatrix:

$$\frac{dy}{dx} = \frac{y(\beta - \gamma x^2)}{x(\alpha - \gamma y^2)}. \quad (39)$$

A completely analogous discussion in the LVCM gives the equation of the separatrix to be Eq. (39), but with γx^2 and

γy^2 replaced by γx and γy , respectively. The solution of this equation is discussed in detail in Appendix A, but in order to simplify the discussion, let us restrict ourselves to the case where $\beta = \alpha$. Then it is not surprising (and is proved in Appendix A) that the equation of the separatrix in the upper quadrant is $y = x$ for both models.

To determine the optimal path, we restrict ourselves to the upper quadrant in the ANPM, since the results in the other quadrants will be identical up to reflections in the x and y axes. To begin, suppose that (x_0, y_0) actually lies on the separatrix (i.e., $y_0 = x_0 \equiv x_{s,0}$ when $\beta = \alpha$). Then since it is clear from Eq. (25) [or alternatively Eq. (23)] that the equations without noise have solutions which have zero action, and since the actions are non-negative, the solutions of Eq. (38) (or the corresponding equations in the LVCM) are solutions of least action. They must therefore be solutions of the second-order Euler-Lagrange equations found from varying the action. This is easy to check by explicit differentiation. When $\beta = \alpha$, trajectories along the separatrix are obtained setting $y(t) = x(t)$ and so solving

$$\dot{x} = \begin{cases} \alpha x - \gamma x^3 & \text{for the ANPM} \\ \alpha x - \gamma x^2 & \text{for the LVCM,} \end{cases} \quad (40)$$

subject to $x(0) = x_{s,0}$. One finds that

$$x_s(t) = \begin{cases} \frac{\sqrt{\alpha x_{s,0}} e^{\alpha t}}{\sqrt{\alpha + \gamma x_{s,0}^2 (e^{2\alpha t} - 1)}} & \text{for the ANPM} \\ \frac{\alpha x_{s,0} e^{\alpha t}}{\alpha + \gamma x_{s,0} (e^{\alpha t} - 1)} & \text{for the LVCM,} \end{cases} \quad (41)$$

where the subscript s is to remind us that this is a solution on the separatrix. Notice that $x_s(t)$ tends to the saddle point as $t \rightarrow \infty$, as required, whichever side of the saddle the initial point is on.

Using the solution (41) for motion along the separatrix as a starting point, we can perform a linearization of the Euler-Lagrange equations about this solution. In this way, we would expect to be able to obtain optimal paths which start at an initial point near the separatrix and end at the saddle point. Therefore, we write [remembering that $y_s(t) = x_s(t)$]

$$x(t) = x_s(t) + \hat{x}(t), \quad y(t) = x_s(t) + \hat{y}(t), \quad (42)$$

and substitute these equations into those for the optimal paths for the ANPM [Eqs. (32) and (33)] and the LVCM [Eqs. (34) and (35)]. Canceling terms using the Euler-Lagrange equation satisfied by $x_s(t)$ and keeping only terms linear in $\hat{x}(t)$ and $\hat{y}(t)$ gives the two sets of equations

$$\ddot{\hat{x}} = (\alpha^2 - 4\alpha\gamma x_s^2 + 7\gamma^2 x_s^4)\hat{x} - 8\gamma x_s^2(\alpha - \gamma x_s^2)\hat{y}, \quad (43)$$

$$\ddot{\hat{y}} = (\alpha^2 - 4\alpha\gamma x_s^2 + 7\gamma^2 x_s^4)\hat{y} - 8\gamma x_s^2(\alpha - \gamma x_s^2)\hat{x} \quad (44)$$

for the ANPM, and

$$\frac{\ddot{\hat{x}}}{x_s} - 2\frac{\dot{x}_s \dot{\hat{x}}}{x_s^2} = \left\{ \frac{\ddot{x}_s}{x_s^2} - 2\frac{\dot{x}_s^2}{x_s^3} + \gamma^2 x_s \right\} \hat{x} - \gamma \frac{\dot{x}_s}{x_s} \hat{y}, \quad (45)$$

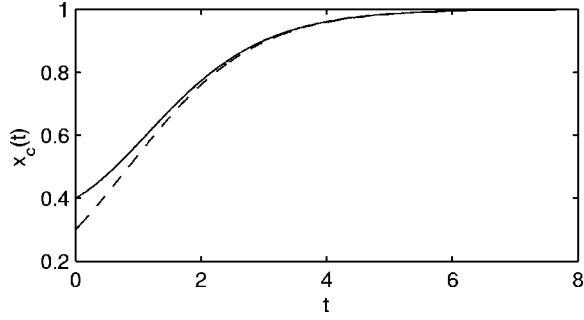


FIG. 2. The x coordinate of the motion along the separatrix for the ANPM (dashed line) and the optimal path within the linear approximation, $x_c(t)$ (solid line) for $(x_0, y_0) = (0.4, 0.2)$ and $\alpha = \beta = \gamma = 1$.

$$\frac{\ddot{y}}{x_s} - 2 \frac{\dot{x}_s \dot{y}}{x_s^2} = \left\{ \frac{\ddot{x}_s}{x_s} - 2 \frac{\dot{x}_s^2}{x_s^3} + \gamma^2 x_s \right\} \hat{y} - \gamma \frac{\dot{x}_s}{x_s} \hat{x} \quad (46)$$

for the LVCM, where we have made use of Eq. (40) to simplify this expression. These equations appear to be complicated, but in fact they can be solved analytically: the explicit forms for these optimal paths within the linear approximation are given in Appendix B. The motion on the separatrix is compared to the linearized solution plus the motion on the separatrix in Fig. 2. The paths begin at different values of x (the separatrix solution begins at the perpendicular projection of the initial point onto the separatrix), but the optimal path approaches the separatrix solution as both approach the saddle point ($x=1$).

The action for the first part of the optimal path from the initial point to the saddle may be found by expanding the classical action around $x_s(t)$,

$$\begin{aligned} S_c = S[\vec{r}_s + \vec{\hat{r}}] &= S[\vec{r}_s] + \sum_{i=1}^2 \int_0^\infty dt \hat{r}_i \left. \frac{\delta S}{\delta r_i(t)} \right|_c \\ &+ \frac{1}{2} \sum_{i,j=1}^2 \int_0^\infty \int_0^\infty dt dt' \hat{r}_i(t) \left. \frac{\delta^2 S}{\delta r_i(t) \delta r_j(t')} \right|_c \hat{r}_j(t'), \end{aligned} \quad (47)$$

to quadratic order. Since $\vec{r}_s(t)$ is a zero-action solution of the extremal equation $\delta S / \delta r_i(t) = 0$, the first two terms on the right-hand side of Eq. (47) vanish, and only the quadratic terms survive. Moreover, by choosing the linear perturbation appropriately, it is shown in Appendix B that $\hat{x}(t) = -\hat{y}(t)$, and in Appendix C that

$$S_c = S(x_0 - y_0)^2, \quad (48)$$

where S is given by

$$S = \frac{(\alpha - \gamma x_{s,0}^2)^2}{4 \left[(\alpha - \gamma x_{s,0}^2) - \gamma x_{s,0}^2 \ln \left(\frac{\alpha}{\gamma x_{s,0}^2} \right) \right]} \quad (49)$$

for the ANPM and

$$S = \frac{(\alpha - \gamma x_{s,0}^2)^2}{8 x_{s,0}^2 \left[\alpha \ln \left(\frac{\alpha}{\gamma x_{s,0}^2} \right) - (\alpha - \gamma x_{s,0}^2) \right]} \quad (50)$$

for the LVCM, and where

$$x_{s,0} = \frac{1}{2}(x_0 + y_0). \quad (51)$$

In the above, we have assumed that $T \rightarrow \infty$, so that the first part of the path ends at the saddle point. The results (48)–(50) hold in this limit. However, as we will discuss in the next section, we need to keep T large, but finite, in order to perform the integration over the possible final states. This is achieved by retaining the initial and final conditions $r(0) = r_0$ and $r(T) = r_f$ for the full path, but modifying the conditions on the first part of the path to be $r(0) = z$ and $r(T) = 0$. Here $r(t) \equiv y(t) - x(t)$ is the coordinate transverse to the separatrix, which turns out to be the crucial one in performing the calculation. The quantity z will be defined in Sec. V, but as $T \rightarrow \infty, z \rightarrow r_0$, as it has to. This means that the results found in this current section are changed when T is large but finite, by (i) replacing $S_c = S r_0^2$ in Eq. (48) by $S_c = S z^2$, and (ii) including exponentially small terms in T —which vanish as $T \rightarrow \infty$ —in the expressions given by Eqs. (49) and (50). We will now go on to discuss these points in more detail.

V. RESULTS

In this section, we add the second part of the optimal path—which starts at the saddle point and ends in the final state—to the calculation carried out in Sec. IV, and so obtain an expression for the probability that each final state is selected. We have seen that the ANPM and the LVCM have the same mechanism of state selection, and the calculations in one model bear a close similarity to those in the other. The advantage of the ANPM is, of course, that because it is a potential model, the stochastic dynamics can be thought of as the dynamics of a Brownian particle moving on a two-dimensional surface. It will be useful to keep this picture in mind, and so we will discuss the final calculation of the state-selection probabilities in the context of the ANPM, even though the formalism will also be applicable to the LVCM.

We are assuming that T is large, so as explained in Sec. IV, the path will run from the initial point near the separatrix to a point near the saddle, and then to the final point. The initial and final points are given, but the intermediate point near the saddle is not: only in the limit $T \rightarrow \infty$ does the path reach the saddle. The optimal paths in the $T \rightarrow \infty$ limit of the ANPM are sketched in Fig. 3. The gridded surface represents the potential U , while the dark lines show the optimal paths. From a starting point near the separatrix, the path goes to the saddle point. From here, two final states are available, and the paths into both the x and y “valleys” are shown. It will also turn out that one of the integrals over the final position becomes singular in the limit $T \rightarrow \infty$, and so T has to be kept large and finite until the last step of the calculation. The approach we will adopt is based on our experience with a

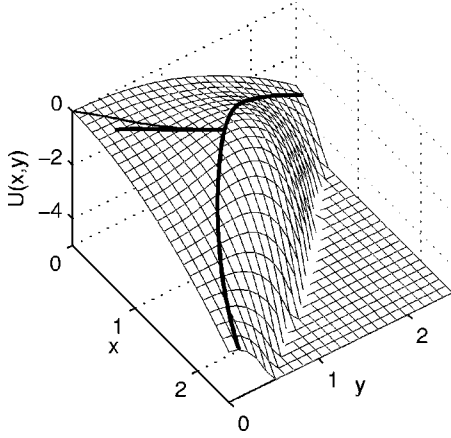


FIG. 3. Representation of the potential U . The solution of the Euler-Lagrange equations from a point near the separatrix to the saddle is shown, with the two alternative paths from the saddle to the two stable states. The fine line is the separatrix.

similar calculation in a one-dimensional problem [$\dot{x} = -V'(x) + \eta(t)$], and we will follow closely Appendix B of Ref. [15].

We once again will assume that $\alpha = \beta$ so that the equation of the separatrix has the simple form $y = x$. Then we define coordinates parallel and perpendicular to the separatrix by

$$r \equiv y - x, \quad s \equiv \frac{1}{2}(x + y) - \sqrt{\frac{\alpha}{\gamma}}, \quad (52)$$

so that the origin is moved to the saddle point. We now pick a positive value of r , which we denote by R , which is far enough from the separatrix so that once the system has crossed the line $r = R$, there is negligible probability of it crossing back over the separatrix and ending up in the x valley. Thus the probability that the system has selected states in the y valley is

$$P(R, T | x_0, y_0, 0) = \int ds_f \int_R^\infty dr_f P(r_f, s_f, T | x_0, y_0, 0), \quad (53)$$

where the integration over the final states (x_f, y_f) has been converted into an integral over the final states (r_f, s_f) in the y valley. The integration over all allowed s_f will be relatively straightforward. The integration over the r_f is more subtle, since it is clearly this integration that is crucial in determining the probability that the system picks its final state in the y valley, so we will carry out this integration first. To do this, let us write the division of the optimal path for motion in the r direction explicitly as the sum of two parts,

$$r(t) = r_1(t; z) + r_2(t; r_f). \quad (54)$$

Here $r_1(t)$ contains the first part of the path to the vicinity of the saddle point and $r_2(t)$ the second part of the path from the vicinity of the saddle point to the final state. For $t \ll T$ (before the saddle point is reached), r_2 is negligible and the solution only consists of r_1 . For t very close to T (after leaving the saddle point), r_1 is negligible and the solution only consists of r_2 . For the vast majority of the time, the system is near the

saddle, so $r(t) \approx 0$ and both terms (r_1 and r_2) are negligible. The initial point of r_1 will not be exactly at r_0 for finite T , with the difference being included in r_2 . The initial and final conditions for the two parts are therefore

$$r_1(0) = z, \quad r_1(T) = 0, \quad (55)$$

$$r_2(0) = r_0 - z, \quad r_2(T) = r_f. \quad (56)$$

The offset $r_2(0)$ can be thought of as the value of r at some intermediate time, when the path is close to the saddle. It is included in r_2 so that we can impose the condition $r_1(T) = 0$, which allows us to use the action for the first part of the path as calculated in Sec. IV. For finite T , $r_2(0; r_f)$ (the initial point of r_2) is nonzero, but as $T \rightarrow \infty$, $r_2(0; r_f) \rightarrow 0$, so $z \rightarrow r_0$ in this limit. Since the two parts of the optimal path are widely separated, the action for the entire path is just the sum of the two separate parts. However, the action of the second part is zero, since this is a “downhill” solution: it is of the form (38) corresponding to a solution of the original set of equations but without noise. Thus the action only comes from the first part of the path. However, this path has to be solved subject to $r_1(0, z) = z$ (by definition) and $r_1(T, z) = 0$ [since we have constructed r_1 and r_2 to ensure this: $r_2(T; r_f) = r(T)$]. This gives the action calculated in the last section (up to exponentially small corrections), except that r_0 must be replaced by z at finite T , that is, $S_c = Sz^2$. Therefore, the probability that the system selects final states in the y valley is found by calculating

$$P(R, T | x_0, y_0, 0) \sim \int ds_f \int_R^\infty dr_f \exp\{-Sz^2/D\}. \quad (57)$$

If we consider T to be fixed at some finite value, then z can be thought of as a function of r_f ; the value of the offset will vary depending on the final point. Now we see why we need to keep T finite. If $T \rightarrow \infty$, z reaches r_0 and so no longer depends on r_f . We need to keep T finite in order to make a change of variables from r_f to z .

To evaluate the integral (57), we change variables from r_f to z using the transformation

$$z = r_0 - r_2(0; r_f), \quad (58)$$

giving

$$P(R, T | x_0, y_0, 0) \sim \int ds_f \int_{-\infty}^Z dz \exp\{-Sz^2/D\}, \quad (59)$$

where $Z = r_0 - r_2(0; R)$. For very large values of r_f , there is not sufficient time for the path to reach a point very close to the saddle and then move to the final point. The offset becomes larger, and since r_0 is fixed, $|z|$ must increase. In the extreme limit as $r_f \rightarrow \infty$, $z \rightarrow -\infty$. Therefore, the upper limit of infinity for r_f becomes a lower limit of minus infinity for z .

Having made the change of variables, we may now let $T \rightarrow \infty$. Since there is zero chance that the final state of the second path will be at $r_f = R$ at infinite time, $Z = r_0$ in this limit, and the result becomes independent of R , as we would expect,

$$P(x_0, y_0) \sim \int ds_f \int_{-\infty}^{r_0} dz \exp\{-S z^2/D\}. \quad (60)$$

The integrand does not depend on s_f , so this second integration will simply produce a prefactor. There are other prefactors, but as we will see, the leading-order exponential in Eq. (60) is sufficient to give excellent agreement with Monte Carlo simulations. The normalization can be determined by noting that if $x_0=y_0$, the probability in Eq. (60) should be $1/2$, since if the system starts on the separatrix, there is an equal probability that it should end up in the x and y valleys. For $r_0 \neq 0$, the integral in Eq. (60) is an error function and so

$$P(y \text{ valley}) = \frac{1}{2} [1 + \operatorname{erf}(r_0 \sqrt{S/D})], \quad (61)$$

$$\Rightarrow P(x \text{ valley}) = \frac{1}{2} [1 - \operatorname{erf}(r_0 \sqrt{S/D})]. \quad (62)$$

We have been assuming that $r_0 > 0$ (i.e., we start above the separatrix, with $y_0 > x_0$), but if $r_0 < 0$, by a similar set of arguments to those given above, we find that

$$P(x \text{ valley}) = \frac{1}{2} [1 + \operatorname{erf}(|r_0| \sqrt{S/D})], \quad (63)$$

$$\Rightarrow P(y \text{ valley}) = \frac{1}{2} [1 - \operatorname{erf}(|r_0| \sqrt{S/D})]. \quad (64)$$

These can be incorporated into one relation,

$$P_{\pm} = \frac{1}{2} \{1 \pm \operatorname{erf}[\sqrt{S_c(r_0)/D}]\}, \quad (65)$$

where $S_c(r_0) = S r_0^2$ and where the plus or minus sign is taken depending on whether the sign of r in the selected state is the same or different from the sign of r_0 .

An identical line of reasoning applies to the LVCN and thus the result (65) gives the probability of each state being selected both in the ANPM and the LVCN, where S is given by Eq. (49) or Eq. (50) as appropriate. The accuracy of this result may be checked by performing a large number of simulations of the original stochastic model starting in the state (x_0, y_0) and counting the fraction of occasions in which the final state lies in the x valley or the y valley.

In Fig. 4, we see just such a comparison. The probability of selecting the x -valley state derived from a numerical simulation of the LVCN model is compared with the probability calculated using Eq. (65), for a range of initial positions along a line perpendicular to the separatrix. The agreement is very good, even for starting points relatively far from the separatrix. In this example $D=0.01$, but the results remain very good for quite large values of D , as shown in Figs. 5 and 6. For the ANPM, there are four competing states, and as D becomes larger, it becomes possible for the two nonadjacent states to be reached (for starting points in the positive quadrant, these are the negative- x and negative- y valleys). The sum of probabilities to reach these states is also marked in the left-hand plots of Figs. 5 and 6 as open circles, and it is clear that the appearance of these states coincides with the

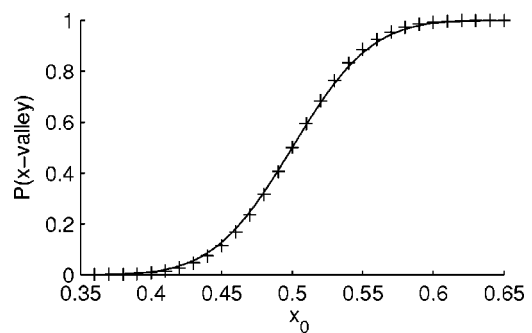


FIG. 4. Probability that the positive- x state is reached in the LVCN, within the linear approximation (solid line) compared with Monte Carlo calculation (+), as a function of starting position along the line $x_0=1-y_0$, when $D=0.01$ and $\alpha=\beta=\gamma=1$.

departure of our calculation from the Monte Carlo values. State selection from points near the origin was considered in Ref. [14], but the selection of the nonadjacent states can be thought of as “escape” over the maximum in the potential near the origin. In systems escaping from a metastable state over a barrier, we would expect escape to become possible when the noise strength reaches some critical value of D , proportional to the barrier height. A crude measure of the height of the “barrier” over which the ANPM system is escaping is ΔV_0 , defined as the difference between the values of the potential at the starting point and at the origin. Figure 7 plots the ratio $\Delta V_0/D_c$ for a variety of starting points in a band of width 0.4 either side of the separatrix (here D_c is the value of D for which the nonadjacent states begin to be accessible). We see that the ratio is indeed relatively constant, and is approximately equal to 7 for this parameter choice. For starting points on the far side of the saddle point from the origin (distances greater than 1.4 in Fig. 7), the “barrier height” is harder to characterize, as there is a minimum (the saddle) between the starting point and the origin, so the ratio $\Delta V_0/D_c$ is less meaningful. Different choices of the parameters α , β , and γ also give a ratio that is constant with starting point, although the value differs. For the LVCN, there are only two possible states, so we do not encounter the same situation. From the right-hand sides of Figs. 5 and 6, it is clear that our results are accurate up to much larger values of D , beyond $D=1$ in this case, when $\alpha=\beta=\gamma=1$.

VI. CONCLUSIONS

In this paper, we have investigated a model of two species in competition with each other in a stochastic environment. In the parameter range of interest, only one species survives in the final state, but there is no *a priori* way of predicting which one it will be: the outcome is stochastic. This is an example of a large class of problems which involve state selection: if there is more than one accessible final state in a dynamical system, what are the probabilities of these being chosen from a given initial state when the system is subject to noise? We described an analytical approach to the calculation of these probabilities and illustrated it on the Lotka-Volterra competition model (LVCN) and on a potential model with additive noise (ANPM). The introduction of this

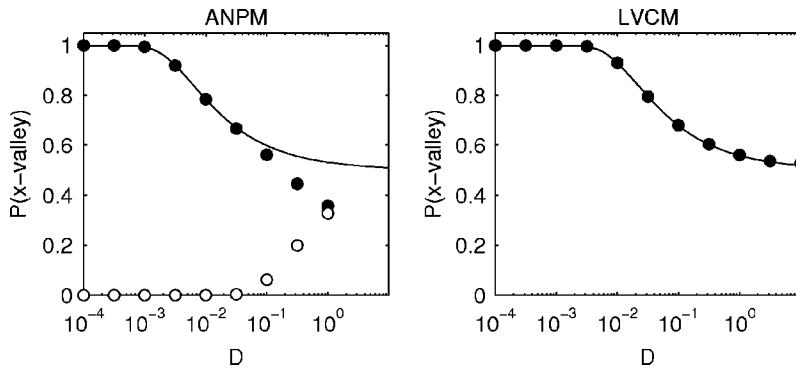


FIG. 5. Probability that the positive- x state is reached, within the linear approximation (solid line), compared with Monte Carlo simulations (black circles) for both ANPM (left) and LVCM (right), as a function of D , for initial position $(x_0, y_0) = (0.4, 0.3)$ and $\alpha = \beta = \gamma = 1$. The open circles are the sum of the probabilities for reaching the states which are on the axes nonadjacent to the starting positions.

latter model served three purposes: (i) it illustrated the fact that the analytical technique which we used has many universal features, and can be applied to many models which show state selection of this kind, (ii) being a potential model, it allowed us to visualize the dynamics far more easily, and (iii) the presence of more than two final states allowed us to observe when the small- D approximation fails. A similar effect is observed for starting points close to the origin. The dynamics of the system in this case are influenced by the unstable point at the origin, and the linearization about the separatrix becomes inaccurate. Starting points near the origin were considered in detail in Ref. [14]. The additive nature of the noise also contrasted with the more complex multiplicative noise of the LVCM.

The calculation was based on the representation of the stochastic differential equations describing the system as path integrals, and the subsequent evaluation of these path integrals using the method of steepest descents for small values of the noise strength. The integrals are dominated by “optimal paths” which can be determined by solving *deterministic* differential equations. These types of calculations are commonplace when studying transitions from one stable state of a dynamical system to another stable state (both made metastable by the addition of noise), but here we have been concerned with quantifying transition probabilities from an arbitrary initial point to a (meta)stable state. The calculation was made easier by the observation that, if the initial state is reasonably far from the separatrix separating the two basins of attraction of the stable states in a system with no noise, then there is little chance of the system crossing over the separatrix. Therefore, in this case the system will select the final state which is in the same basin of attraction as the initial state. It is clear that this will not be the case

for initial points near the separatrix, where there will be a nonzero probability of the system crossing over. How “near” is defined is not so clear, but we found that results which are in excellent agreement with numerical simulations can be obtained by keeping only the leading-order (exponential) term in the steepest-descent calculation and linearizing the equations for the optimal paths about optimal paths which lie entirely on the separatrix. The reasons why using only the leading-order contribution is sufficient to get such good agreement, even for values of D larger than 1, is not at all clear and merits further investigation. It also shows that there are no noise-induced transitions because of changes in stability of fixed points or because of new steady states created at finite D . Such phenomena may occur in systems with multiplicative noise [27–29]. They would not be picked up by the approximations used in this paper, which are valid in the limit $D \rightarrow 0$.

In an earlier paper [15], we discussed the relationship between calculations of the type we have presented here and those carried out using the backward Fokker-Planck equation [30,31]. Although the latter method is considerably simpler to implement for one-dimensional problems, for systems involving two dimensions or more it is much less useful. In fact, the calculation in these cases proceeds by a series of mappings on to the classical mechanics defined by the action S discussed in Sec. III. By contrast, the path-integral method is more directly associated with the original stochastic problem, and the intuition gained by visualization of the optimal paths is frequently helpful.

An important ingredient in the analysis was the observation that the state-selection probabilities become independent of the time interval, T , between the initial and final states if T is sufficiently large that state selection has had a chance to

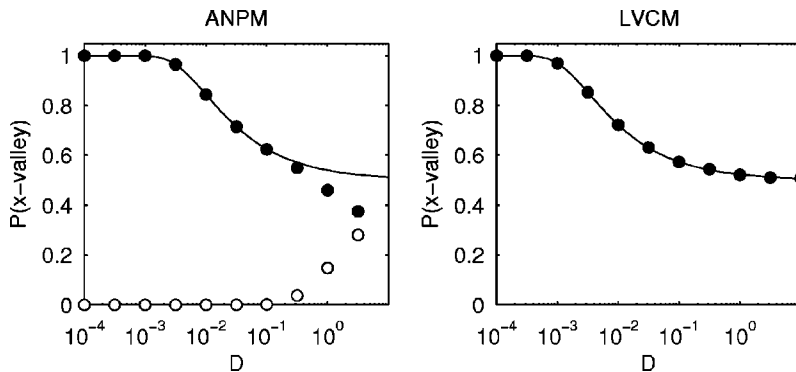


FIG. 6. Probability that the positive- x state is reached, within the linear approximation (solid line), compared with Monte Carlo simulations (black circles) for both ANPM (left) and LVCM (right), as a function of D , for initial position $(x_0, y_0) = (1.3, 1.2)$ and $\alpha = \beta = 0.8, \gamma = 1$. The open circles are the sum of the probabilities for reaching the states which are on the axes nonadjacent to the starting positions.

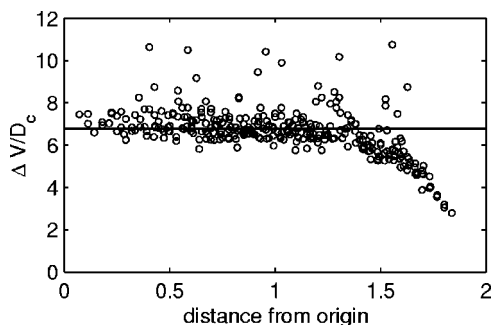


FIG. 7. Ratio of ΔV_0 to D_c for starting points within 0.2 of the separatrix, as a function of the distance of the starting point from the origin. The open circles are based on Monte Carlo simulations of 50 000 runs, as are those in Figs. 5 and 6.

occur. However, the calculation simplifies considerably in the limit $T \rightarrow \infty$, since the optimal path passes through the saddle point, which allows us to break the path down into two distinct parts. The first part of the path runs from the initial point (x_0, y_0) to the saddle point and has a nonzero action if the initial point is not on the separatrix ($x_0 \neq y_0$ in the symmetric case $\alpha = \beta$). The second part has zero action. There is a small technical complication: in order to perform an integral over one of the final positions (r_f), it is necessary to keep T large but finite. This is overcome by reexpressing the initial and final conditions on the entire optimal path [$r(0) = r_0$, $r(T) = r_f$] as initial and final conditions on the first part of the path only [$r_1(0) = z$, $r_1(T) = 0$]. After the change of variable from r_f to z has been carried out in the integral, the limit $T \rightarrow \infty$ may safely be taken.

The method of calculation was illustrated by assuming that the growth rate of both species was equal ($\alpha = \beta$). This implied that the separatrix was simply given by the equation $y = x$. There is no problem performing the calculation when $\alpha \neq \beta$, but much of it has to be carried out numerically because the equation of the separatrix in this case (given in Appendix A) can only be found implicitly. The optimal path on the separatrix can be found by integrating backwards in time from the saddle point (so that the direction along the separatrix is unstable).

The most remarkable aspect of the calculation was the fact that a simple, closed form expression for the state-selection probability could be found which held for values of D as large as 10 (for the range of values of the other parameters of the model which we investigated). This is larger than we would naively have expected and is a much larger value than would be used in practice, since in the construction of the stochastic equations, the effects modeled by the noise terms should be small in relation to the other terms. We were able to identify the reason for the breakdown in the approximation as D increased in the ANPM. This happened at smaller values of D than for the LVPM, and was due to escape from initial states in the positive quadrant to the states lying on the negative x and negative y axes. Since no such states exist for the LVPM (x and y being constrained to be non-negative), this effect is not present in this case. These results were obtained without having to go beyond leading order or beyond the linear approximation about the optimal

path on the separatrix. In addition, no integration had to be carried out to calculate the action of the optimal paths. We expect these features will persist in more complicated problems of this type, such as higher-dimensional systems, and so provide a means of determining state-selection probabilities in a range of situations.

ACKNOWLEDGMENTS

We wish to thank Nick Barton, Roger Nisbet, and Michael Turelli for useful discussions. G.B. thanks the New Zealand Tertiary Education Commission for financial support. Support from the Complex Systems Group, Northwestern University, is gratefully acknowledged. Support from the NSF-IGERT program ‘‘Dynamics of Complex Systems in Science and Engineering’’ (Grant No. DGE-9987577) at Northwestern University is also acknowledged.

APPENDIX A: EQUATION OF THE SEPARATRIX

In this appendix, we determine the equation of the separatrix both for the ANPM and the LVCM, and also the equation of the optimal paths in both models which start on the separatrix and end at the saddle point.

As discussed in Sec. IV, the equations of the optimal paths which stay on the separatrix are simply the original stochastic equations, but without the noise. These equations are first-order equations which can be shown to satisfy the second-order Euler-Lagrange equations obtained from a variation of the appropriate action. These equations for the ANPM were given in Sec. IV [Eq. (38)], and for the LVCM they are

$$\dot{x} = \alpha x - \gamma xy, \quad \dot{y} = \beta y - \gamma xy. \quad (\text{A1})$$

Clearly these two sets of equations are very closely related: if we substitute $x'(\tau) = x^2(t)$ and $y'(\tau) = y^2(t)$, where $\tau = 2t$, in Eq. (38), we obtain Eq. (A1). So if we can solve one set of equations, we can solve the other. Therefore, we will concentrate on those given by Eq. (A1).

Let us first simplify the equations by introducing new variables X and Y through

$$x(t) = \frac{\beta X(t)}{\gamma}, \quad y(t) = \frac{\alpha Y(t)}{\gamma}, \quad (\text{A2})$$

so that Eq. (A1) now reads

$$\dot{X} = \alpha X(1 - Y), \quad \dot{Y} = \beta Y(1 - X). \quad (\text{A3})$$

The saddle point is now at $(X^*, Y^*) = (1, 1)$ and the equation of the separatrix is

$$\frac{dY}{dX} = \frac{\beta Y(1 - X)}{\alpha X(1 - Y)}. \quad (\text{A4})$$

Solving this equation subject to the condition that $Y = 1$ when $X = 1$ gives

$$[X \exp(1 - X)]^\beta = [Y \exp(1 - Y)]^\alpha. \quad (\text{A5})$$

When $\beta = \alpha$, this equation reduces to $Xe^{-X} = Ye^{-Y}$. The solutions of the equation $f(X) = f(Y)$, where $f(\zeta) = e^{\ln \zeta - \zeta}$, may be

investigated by considering the inverse of the function $g(\zeta) = (\zeta - 1) - \ln \zeta \geq 0$. The solution we require is the one which lies in the sectors $X, Y < 1$ and $X, Y > 1$ and is simply $X = Y$. The equation of the optimal path is seen from Eq. (A3) to satisfy $\dot{X} = \alpha X(1 - X)$, which is easily solved to give

$$X_s(t) = \frac{X_{s,0} e^{\alpha t}}{1 + X_{s,0}(e^{\alpha t} - 1)}, \quad (\text{A6})$$

where $X_0 = Y_0 \equiv X_{s,0}$ is the starting point.

When $\alpha \neq \beta$, new variables can be defined by

$$\rho = [X \exp(1 - X)]^\beta, \quad \sigma = [Y \exp(1 - Y)]^\alpha, \quad (\text{A7})$$

so that the equation of the separatrix is $\rho = \sigma$, the saddle point is again $(1, 1)$, and $\rho(t) = \sigma(t)$ for the optimal path on the separatrix. However, we have not found a differential equation for $\rho(t)$ which is simple enough to solve, and so the optimal path has to be found numerically in this case. This is easy enough to do: by reversing the time, and starting from a point arbitrarily close to the saddle point, the direction along the separatrix is now unstable and the solution to a given initial (now final) point on the separatrix can be determined. A similar calculation leads to equations for the ANPM similar to Eqs. (A6) and (A7).

APPENDIX B: LINEARIZATION NEAR THE SEPARATRIX

In Sec. IV, we obtained equations for the optimal paths which start near the separatrix by linearizing about optimal paths which start on the separatrix. These linear deviations satisfy Eqs. (43) and (44) in the case of the ANPM and Eqs. (45) and (46) in the case of the LVCM. In this appendix, we explicitly solve these equations.

In both cases, the equations can be decoupled by defining new variables

$$r(t) = \hat{y}(t) - \hat{x}(t), \quad s(t) = \frac{1}{2}[\hat{x}(t) + \hat{y}(t)]. \quad (\text{B1})$$

The equations in terms of these new variables are now

$$\dot{r} = (\alpha^2 + 4\alpha\gamma x_s^2 - \gamma^2 x_s^4)r, \quad (\text{B2})$$

$$\dot{s} = (\alpha^2 - 12\alpha\gamma x_s^2 + 15\gamma^2 x_s^4)s \quad (\text{B3})$$

for the ANPM, and

$$\frac{\ddot{r}}{x_s} - 2\frac{\dot{x}_s \dot{r}}{x_s^2} = \left\{ \frac{\ddot{x}_s}{x_s^2} - 2\frac{\dot{x}_s^2}{x_s^3} + \gamma^2 x_s + \gamma \frac{\dot{x}_s}{x_s} \right\} r, \quad (\text{B4})$$

$$\frac{\ddot{s}}{x_s} - 2\frac{\dot{x}_s \dot{s}}{x_s^2} = \left\{ \frac{\ddot{x}_s}{x_s^2} - 2\frac{\dot{x}_s^2}{x_s^3} + \gamma^2 x_s - \gamma \frac{\dot{x}_s}{x_s} \right\} s \quad (\text{B5})$$

for the LVCM. To determine the initial conditions in terms of r and s , let us first note that we may also define them as

$$r(t) = y(t) - x(t), \quad s(t) = \frac{1}{2}[x(t) + y(t)] - x_s(t). \quad (\text{B6})$$

The variable $r(t)$ corresponds to motion perpendicular to the separatrix and $s(t)$ to motion parallel to the separatrix.

In the original formulation of the problem, there are two initial conditions, $x(0) = x_0$ and $y(0) = y_0$, but we now have three possible initial parameters: $r_0 = r(0)$, $s_0 = s(0)$, and $x_{s,0} = x_s(0)$. We are free to choose one of them however we wish, so long as the remaining two are then chosen so as to satisfy $x(0) = x_0$ and $y(0) = y_0$. If we think of the initial point (x_0, y_0) as a perturbation about the separatrix, we are effectively free to choose the direction of the perturbation from $(x_{s,0}, x_{s,0})$. It would seem sensible to choose $x_{s,0}$ so that the perturbation is as small as possible—that is, perpendicular to the separatrix. So we choose $s_0 = 0$, which means we must have $x_{s,0} = \frac{1}{2}(x_0 + y_0)$ and $r_0 = y_0 - x_0$. As we will see later, this choice of linearization leads to significant simplifications.

The equations for r and s may be further rationalized by introducing new variables

$$s(t) = x_s f(t), \quad r(t) = x_s g(t). \quad (\text{B7})$$

For the ANPM, we have

$$\ddot{f} + \frac{\dot{\phi}}{\phi} \dot{f} = (3\phi^2 - 2\phi)f, \quad (\text{B8})$$

$$\ddot{g} + \frac{\dot{\phi}}{\phi} \dot{g} = (-\phi^2 + 2\phi)g, \quad (\text{B9})$$

where $\phi = \gamma x_s^2 / \alpha$ and the time derivatives are now with respect to $\tau = 2\alpha t$. For the LVCM, we have

$$\ddot{f} = (2\psi^2 - \psi)f, \quad (\text{B10})$$

$$\ddot{g} = \psi g, \quad (\text{B11})$$

where $\psi = \gamma x_s / \alpha$ and the time derivatives are now with respect to $\tau = \alpha t$.

We now make one last transformation. We introduce a new independent variable

$$\mu = \frac{1}{1 + Ae^\tau}, \quad (\text{B12})$$

where

$$A = \begin{cases} \frac{\gamma x_{s,0}^2}{\alpha - \gamma x_{s,0}^2} & \text{for the ANPM} \\ \frac{\gamma x_{s,0}}{\alpha - \gamma x_{s,0}} & \text{for the LVCM.} \end{cases} \quad (\text{B13})$$

Then $\phi = 1 - \mu$ and $\dot{\phi} / \phi = \mu$, and also $\psi = 1 - \mu$. In addition, we introduce new dependent variables

$$f(\tau) = \mu F(\mu), \quad g(\tau) = \mu G(\mu). \quad (\text{B14})$$

Substituting these changes of variables into the equations for f and g , and canceling terms proportional to $(1 - \mu)$ and μ^2 from the resulting differential equations ($\mu = 1$ only when $t = 0$ and $\mu \neq 0$ for finite t), we find

$$\mu(1 - \mu) \frac{d^2 F}{d\mu^2} + (3 - 5\mu) \frac{dF}{d\mu} = 0, \quad (\text{B15})$$

$$\mu(1-\mu)\frac{d^2G}{d\mu^2} + (3-5\mu)\frac{dG}{d\mu} - 4G = 0 \quad (\text{B16})$$

for the ANPM and

$$\mu(1-\mu)\frac{d^2F}{d\mu^2} + (3-4\mu)\frac{dF}{d\mu} = 0, \quad (\text{B17})$$

$$\mu(1-\mu)\frac{d^2G}{d\mu^2} + (3-4\mu)\frac{dG}{d\mu} - 2G = 0 \quad (\text{B18})$$

for the LVCM. These are hypergeometric equations, but fortunately the solutions correspond to degenerate cases and can all be expressed in terms of elementary functions. Independent solutions are

$$F_1(\mu) = 1, \quad F_2(\mu) = 3 \ln\left(\frac{\mu}{1-\mu}\right) + \frac{1}{1-\mu} - \frac{1}{2\mu^2} - \frac{2}{\mu}, \quad (\text{B19})$$

$$G_1(\mu) = \frac{1}{\mu^2} \ln(1-\mu) + \frac{1}{\mu(1-\mu)}, \quad G_2(\mu) = \frac{1}{\mu^2} \quad (\text{B20})$$

for the ANPM and

$$F_1(\mu) = 1, \quad F_2(\mu) = -2 \ln\left(\frac{\mu}{1-\mu}\right) + \frac{1}{\mu^2} + \frac{2}{\mu}, \quad (\text{B21})$$

$$G_1(\mu) = \frac{1}{\mu^2} \ln(1-\mu) + \frac{1}{\mu}, \quad G_2(\mu) = \frac{1}{\mu^2} \quad (\text{B22})$$

for the LVCM.

We require that both $\hat{x}(t)$ and $\hat{y}(t)$ tend to zero as $t \rightarrow \infty$, so that the end point of the path is at the saddle point. This implies that only the solutions $F_1(\mu)$ and $G_1(\mu)$ in the above set of solutions are allowed. The solutions for $s(t)$ have the especially simple forms

$$s(t) = \begin{cases} B_1 x_s (\alpha - \gamma x_s^2) / \alpha & \text{for the ANPM} \\ B_2 x_s (\alpha - \gamma x_s) / \alpha & \text{for the LVCM,} \end{cases} \quad (\text{B23})$$

where B_1 and B_2 are constants. Implementing the initial condition $s(0)=0$ gives $B_1=B_2=0$ and so $s(t) \equiv 0$. This shows that our choice of perturbation means that motion is such that $\hat{x}(t) = -\hat{y}(t)$, which greatly simplifies the analysis.

The remaining solution is given by

$$r(t) = \begin{cases} C\{[\alpha x_s / (\alpha - \gamma x_s^2)] \ln(\gamma x_s^2 / \alpha) + [\alpha / (\gamma x_s)]\} & \text{for the ANPM} \\ D\{[\alpha x_s / (\alpha - \gamma x_s)] \ln(\gamma x_s / \alpha) + x_s\} & \text{for the LVCM,} \end{cases} \quad (\text{B24})$$

where C and D are constants. Since $r(0)=r_0=y_0-x_0$, we identify the constants C and D as

$$C = r_0 \{[\alpha x_{s,0} / (\alpha - \gamma x_{s,0}^2)] \ln(\gamma x_{s,0}^2 / \alpha) + [\alpha / (\gamma x_{s,0})]\}^{-1}, \quad (\text{B25})$$

$$D = r_0 \{[\alpha x_{s,0} / (\alpha - \gamma x_{s,0})] \ln(\gamma x_{s,0} / \alpha) + x_{s,0}\}^{-1}. \quad (\text{B26})$$

Finally we note that, since $\hat{x}(t) = -\hat{y}(t)$, $r(t) = -2\hat{x}(t) = 2\hat{y}(t)$.

APPENDIX C: CALCULATION OF THE ACTION

Having determined the analytic form for the portion of the optimal path from the initial state to the separatrix in Appendix B, we will now determine the action of this solution. It will turn out that it can be calculated without carrying out any further integrals. The action of the path from the saddle point to the final state is zero, so the action calculated in this appendix is the total action.

To calculate the action for the ANPM (25), we need to find $\dot{x} + \partial V / \partial x$ and $\dot{y} + \partial V / \partial y$. Substituting $x = x_s + \hat{x}$, $y = x_s + \hat{y}$, and using the fact that $x_s(t)$ satisfies Eq. (40) and $\hat{y}(t) = -\hat{x}(t) = r(t)/2$,

$$\left(\dot{x} + \frac{\partial V}{\partial x}\right) = -\left(\dot{y} + \frac{\partial V}{\partial y}\right) = -\frac{1}{2}\{\dot{r} - [\alpha + \gamma x_s^2]r\} \quad (\text{C1})$$

to linear order. For the LVCM, an analogous calculation gives

$$\left(\frac{\dot{x}}{x} - \alpha + \gamma y\right) = -\left(\frac{\dot{y}}{y} - \beta + \gamma x\right) = -\frac{1}{2}\left\{\frac{d}{dt}\left(\frac{r}{x_s}\right) - \gamma r\right\}, \quad (\text{C2})$$

again to linear order. We therefore find the classical action for the first part of the path in the ANPM to be

$$S_c = \frac{1}{8} \int_0^T dt [\dot{r} - (\alpha + \gamma x_s^2)r]^2, \quad (\text{C3})$$

and for the LVCM to be

$$S_c = \frac{1}{8} \int_0^T dt [g - \gamma x_s g]^2, \quad (\text{C4})$$

where $g(t)$ is defined by Eq. (B7). Multiplying out the square in the integrands and integrating by parts yields new integrals which are identically zero. To prove this, Eq. (40) for the x_s has to be used, as well as Eq. (B2) for r and Eq. (B11)

for g . Only the boundary terms obtained through integration by parts remain,

$$S_c = \begin{cases} \frac{1}{8}[r\dot{r} - (\alpha + \gamma x_s^2)r^2]_0^T & \text{for the ANPM} \\ \frac{1}{8}[g\dot{g} - \gamma x_s g^2]_0^T & \text{for the LVCM.} \end{cases} \quad (C5)$$

Both r and g vanish at the upper limit, and also we may show by direct differentiation of Eq. (B24) that

$$\dot{r} - (\alpha + \gamma x_s^2)r = -\frac{2\alpha C(\alpha - \gamma x_s^2)}{\gamma x_s} \quad (C6)$$

for the ANPM and

$$\dot{g} - \gamma x_s g = D(\alpha - \gamma x_s) \quad (C7)$$

for the LVCM. Therefore, we find that

$$S_c = \frac{(\alpha - \gamma x_{s,0}^2)^2 r_0^2}{4 \left[(\alpha - \gamma x_{s,0}^2) - \gamma x_{s,0}^2 \ln \left(\frac{\alpha}{\gamma x_{s,0}^2} \right) \right]} \quad (C8)$$

for the ANPM and

$$S_c = \frac{(\alpha - \gamma x_{s,0})^2 r_0^2}{8x_{s,0}^2 \left[\alpha \ln \left(\frac{\alpha}{\gamma x_{s,0}} \right) - (\alpha - \gamma x_{s,0}) \right]} \quad (C9)$$

for the LVCM.

-
- [1] E. C. Pielou, *Mathematical Ecology*, 2nd ed. (Wiley, New York, 1977).
 - [2] R. M. May, *Model Ecosystems* (Princeton University Press, Princeton, NJ, 1973), Chap. 5.
 - [3] J. M. G. Vilar and R. V. Sole, *Phys. Rev. Lett.* **80**, 4099 (1998).
 - [4] C. Neuhauser and S. W. Pascala, *Ann. Appl. Probab.* **9**, 1226 (1999).
 - [5] M. Heino, J. Ripa, and V. Kaitala, *Ecography* **23**, 177 (2000).
 - [6] M. F. Dimentberg, *Phys. Rev. E* **65**, 036204 (2002).
 - [7] B. Spagnolo and A. La Barbera, *Physica A* **315**, 114 (2002).
 - [8] M. C. Wichmann, K. Johst, K. A. Moloney, C. Wissel, and F. Jeltsch, *Ecol. Modell.* **167**, 221 (2003).
 - [9] C. Escudero, J. Buceta, F.-J. de la Rubia, and K. Lindenberg, *Phys. Rev. E* **69**, 021908 (2004).
 - [10] R. Mankin, A. Sauga, A. Ainsaar, A. Haljas, and K. Paunel, *Phys. Rev. E* **69**, 061106 (2004).
 - [11] D. Valenti, A. Fiasconaro, and B. Spagnolo, *Acta Phys. Pol. B* **35**, 1481 (2004).
 - [12] S. J. B. Einchcomb and A. J. McKane, in *Fluctuations and Order*, edited by M. Millonas (Springer-Verlag, New York, 1996), p. 139.
 - [13] M. B. Tarlie and A. J. McKane, *J. Phys. A* **31**, L71 (1998).
 - [14] A. J. McKane and M. B. Tarlie, *Phys. Rev. E* **64**, 026116 (2001).
 - [15] A. J. McKane and M. B. Tarlie, *Phys. Rev. E* **69**, 041106 (2004).
 - [16] F. Reif, *Statistical and Thermal Physics* (McGraw-Hill, New York, 1965), Chap. 15.
 - [17] L. E. Reichl, *A Modern Course in Statistical Physics* (Wiley, New York, 1998).
 - [18] R. M. May, *Am. Nat.* **107**, 621 (1973).
 - [19] N. G. van Kampen, *J. Stat. Phys.* **24**, 175 (1981).
 - [20] M. Turelli, *Theor. Popul. Biol.* **12**, 140 (1977).
 - [21] R. P. Feynman and A. R. Hibbs, *Quantum Mechanics and Path Integrals* (McGraw-Hill, New York, 1965), Chap. 12.
 - [22] R. Graham, in *Quantum Statistics in Optics and Solid-State Physics*, Springer Tracts in Modern Physics Vol. 66 (Springer-Verlag, New York, 1973).
 - [23] R. Graham, in *Fluctuations, Instabilities and Phase Transitions*, edited by T. Riste (Plenum, New York, 1975).
 - [24] J. Zinn-Justin, *Quantum Field Theory and Critical Phenomena* (Oxford University Press, New York, 2002).
 - [25] C. Lanczos, *The Variational Principles of Mechanics* (University of Toronto Press, Toronto, 1970).
 - [26] L. Onsager and S. Machlup, *Phys. Rev.* **91**, 1512 (1953).
 - [27] L. Arnold, W. Horsthemke, and R. Lefever, *Z. Phys. B* **29**, 367 (1978).
 - [28] A. S. Mikhailov, *Z. Phys. B: Condens. Matter* **41**, 277 (1981).
 - [29] W. Horsthemke and R. Lefever, *Noise-Induced Transitions* (Springer-Verlag, Berlin, 1984).
 - [30] M. Mangel and D. Ludwig, *SIAM (Soc. Ind. Appl. Math.) J. Appl. Math.* **33**, 256 (1977).
 - [31] M. Mangel, *Theor. Popul. Biol.* **45**, 16 (1994).